



SHAKING TABLE TEST AND ANALYSIS OF REINFORCED CONCRETE WALLS

Tomoya MATSUI¹, Toshimi KABEYASAWA², Atsushi KOTO³,
Hiroshi KURAMOTO⁴ and Ichiro NAGASHIMA⁵

SUMMARY

A dynamic experiment of two reinforced concrete walls was carried out in June and July, 2002, as a preliminary test towards a full-scale dynamic test of a building in 2005. Objectives of the study are to obtain seismic performances of the walls under dynamic loading, such as hysteretic behavior, deformability and failure mechanism, and to verify a macro member model of shear wall based on the test data.

The two specimens were identical and one-third scale model of a plane shear wall with boundary columns representing lower two stories in a six-story wall-frame building. Upper stories were modeled with equivalent mass of steel weight above the concrete slab at the top of the wall. Only the height to the center of the mass from the base was changed between the two specimens simulating different modes of the lateral load distributions in the proto-type building. The two specimens were subjected to the same series of earthquake motions, the intensity of which were amplified gradually, until up to failure.

The first specimen Wall-A with the lower mass height failed in shear after flexural yielding as was expected from the calculated shear strength, which was close to the flexural strength. The second specimen Wall-B, the calculated shear strength of which is apparently higher than the flexural strength, also failed in shear under the smaller input motion level.

From the analysis on the hysteretic energy dissipation, this is due to many cyclic responses of longer period in Wall-B after yielding so that the total input energy was accumulated, although the maximum deformation amplitudes top of wall were not much larger than those of Wall-A. The envelope curve obtained from the experiment were simulated well until up to beginning of sharp deterioration of shear strength by a macro member model, which includes the effect of concrete strength softening under combined two-dimensional stresses.

¹ Graduate Students, School of Engineering, The University of Tokyo, Japan. Email: matsui@eri.u-tokyo.ac.jp

² Professor, Earthquake Research Institute, The University of Tokyo, Japan. Email: kabe@eri.u-tokyo.ac.jp

³ National Research Institute for Earth Science and Disaster Prevention, Japan. Email: kato@bosai.go.jp

⁴ Professor, Toyohashi University of Technology, Japan. Email: kura@tutrp.tut.ac.jp

⁵ Engineer, Technology center, Taisei Corporation, Japan. Email: nagashima@sakura.taisei.co.jp

INTRODUCTION

Guidelines for Performance Evaluation of Earthquake Resistant Reinforced Concrete Building (Draft) [1] was published in Japan, January 2004. Three limit states are prescribed in the guidelines for seismic performance objectives: serviceability, restorability, and safety. The safety limit state is defined conceptually as the near collapse at the loss of the gravity loading carrying capacity, although the inelastic deformation limit adopted for design is still conservative, because the accuracy of evaluation is not enough. The hysteretic behavior beyond the peak strength including the strength deterioration should be evaluated by ultimate state for earthquake is evaluated as correctly as possible. However, the analytical model so far, especially for shear wall members, could not simulate the behavior with strength deterioration with satisfactory accuracy so that it is still necessary to develop a rational model of shear wall for analytical evaluation of the safety limit state with experimental verification.

In this study, a dynamic experiment of two reinforced concrete walls was carried out in order to understand collapse mechanism, the hysteresis behavior, the deformability of the shear wall under dynamic loading, and to verify a macro member model of shear wall based on the test data. The results of the test are reported and the analytical simulation of the test with the macro member model is described.

DESCRIPTION OF TEST

Specimen

In this experiments, the two specimens were identical and 1/3 scale model of a plane shear wall with boundary columns representing lower stories in a six-story wall-frame building. Since it aims at acquiring the data of simple shear walls, detail of specimens were made as shown in Fig.1, and out of plane deformation is restrained by setting steel frame as shown in Fig.2.

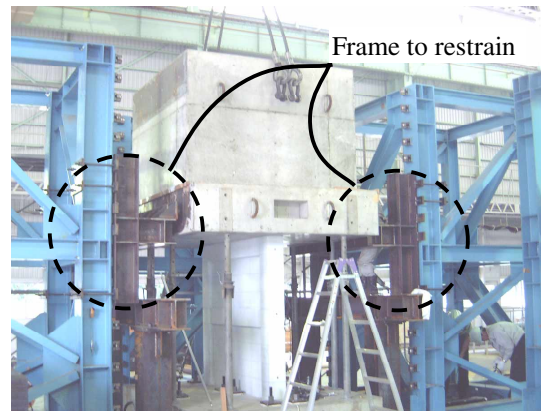
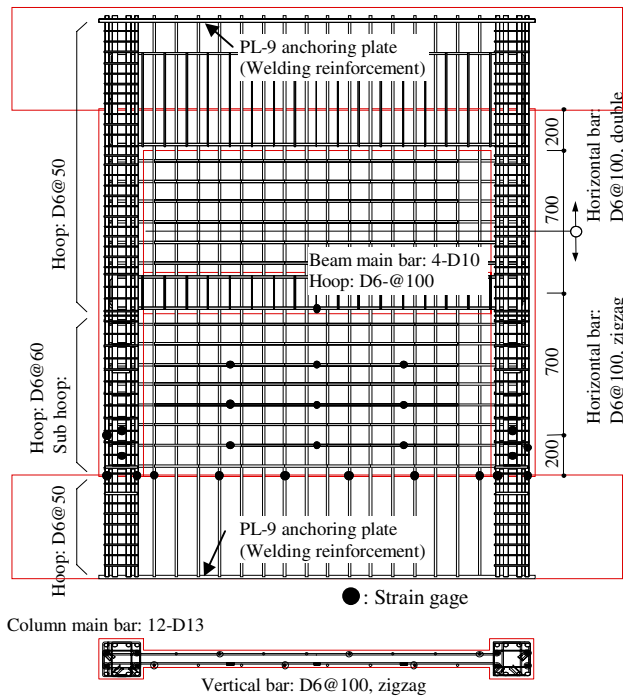


Fig.2. View of specimen under setting

Fig.1. Reinforcement details of wall and strain gage setting points

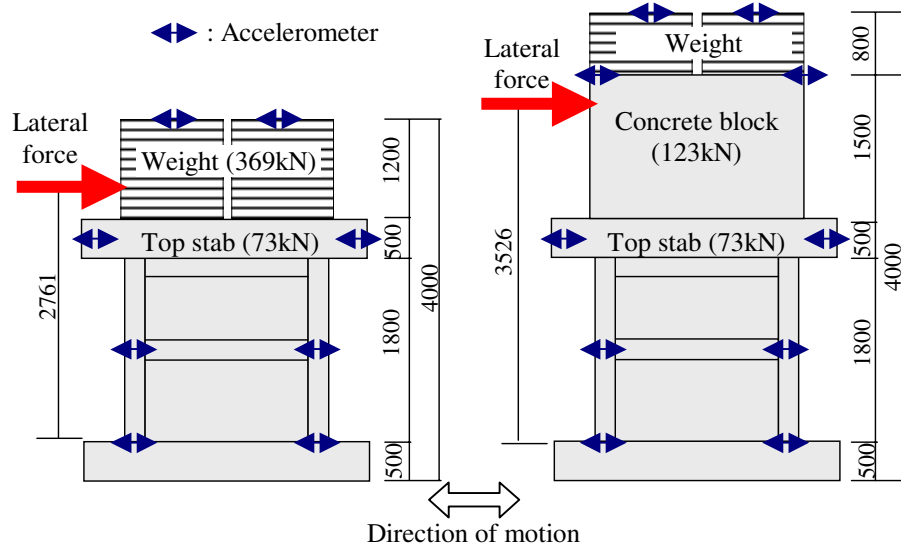


Fig.3. Position of inertia force and accelerometer

Table 1. Section details of member (unit: mm)

		1F	2F
Column	B × D	200 × 200	
	Main bar	12-D13(p _g =3.8%)	
	Hoop	2-D6@60 (p _w =0.53%)	2-D6@50 (p _w =0.64%)
	Sub hoop	2-D6@120 (p _w =0.27%)	—
Beam	B × D	150 × 200	200 × 500 (included 300 in top slab)
	Main bar	4-D10(p _t =0.54%)	
	Hoop	2-D6@100(p _w =0.42%)	
Wall	Thickness	80	
	Vertical bar	D6@100(p _s =0.4%)	2-D6@100(p _s =0.8%) (top 400mm) D6@100(p _s =0.4%)
	Horizontal bar	D6@100(p _s =0.4%)	

Table 2. Material properties of concrete

Specimen		Age (Days)	σ_B (N/mm ²)	ϵ (μ)	E_c (kN/mm ²)	ν	σ_t (N/mm ²)
Specimen A (Shear failure type)	1st story wall	40	26.4	1770	24.4	0.19	2.62
	2nd story wall	32	30.0	1861	25.4	0.19	2.69
Specimen B (Bending failure type)	1st story wall	48	25.2	1811	24.8	0.18	2.47
	2nd story wall	40	29.6	1828	26.2	0.19	2.48

σ_B : cylinder strength, ϵ : strain at σ_B , E_c : $\sigma_B/3$ secant modulus, ν : Poisson's ratio, σ_t : tension strength

Table 3. Material properties of steels

		σ_y (N/mm ²)	ϵ_y (μ)	E_s (kN/mm ²)	σ_t (N/mm ²)	Elongation (%)
D6 (SD295A)	Wall, Hoop of column and beam	377	1952	196	493	29.4
D10 (SD295A)	Main bar of beam	366	2018	181	503	28.0
D13 (SD390)	Main bar of column	434	2538	186	605	22.8

σ_y : yielding strength, ϵ_y : yielding strain, E_s : Young's modulus, σ_t : tension strength

Only the height to the center of the mass (442kN) from the base was changed between the two specimens to simulate the effect on the collapse mechanism, because the effective height of dynamic lateral load may change to the change in distribution of the mass (fig.3). And, preceding shear collapse type wall (Wall-A) and preceding flexural yield type wall (Wall-B) were prepared. Shear span ratio (M/Ql_w) are calculated 1.38(Wall-A) and 1.75(Wall-B). Section detail and bar arrangement drawing of members are shown in Table.1. Material property of concrete and reinforcement are shown in Table 2 and Table 3.

Similitude low

In order to satisfy axial stress equivalent to first-story shear wall of six-story structure, addition weight on specimen was required except for own weight. Steel weight was added, top weight make 442kN, as a result target similitude low was nearly satisfied. Therefore input acceleration acting specimens corresponding to the effect to the structure of original design, applying similitude low of time, the duration time of the input base motion was scaled by 1/ the square root 3.

Measurement method

Accelerations were measured 30 ingredients, mainly base motion direction on top weight, 3-direction on top slab, beam of first-story and foundation slab (Fig.3.). Displacements were measured lateral and vertical displacement on top slab and perimeter column, axial displacement of perimeter column divided into fore parts, and displacement of wall with displacement transducers (Fig.4). Strains of reinforcement were measured main position of reinforcement of column, beam and wall with strain gauges (Fig.1.). Sampling rate of measuring was 2000 Hz, respectively.

Base motion input plan

The two specimens were subjected to the same series base motion with recorded motion selected five, as shown in Table 4. : TOH, Miyagi-ken Oki

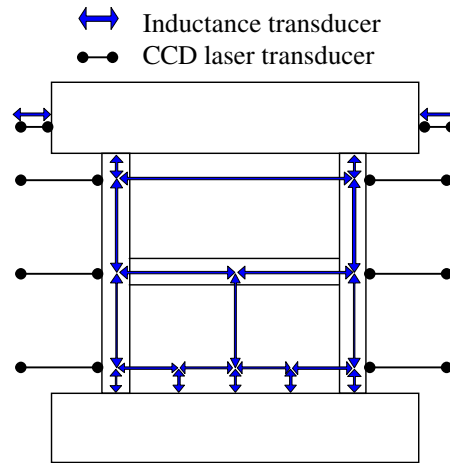


Fig.4. Transducer setting points

Table 4. Base motion input plan

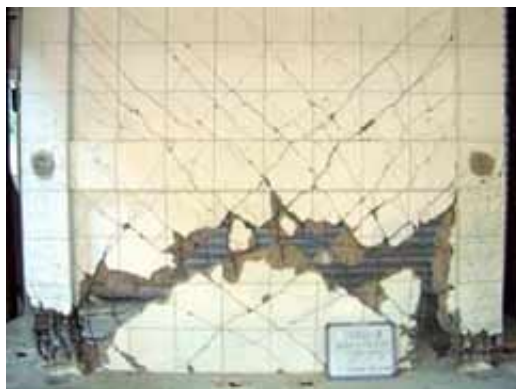
	Maximum target velocity	Earthquake data	Ratio to the prototype	Maximum acceleration of prototype	Maximum velocity of prototype	Maximum acceleration input of specimen	Maximum velocity input of specimen	Duration
	(kine)			(gal)	(kine)	(gal)	(kine)	(sec)
Run1	25	TOH	0.6	258.2	40.9	154.9	14.4	26.6
Run2	37	ELC	1.1	341.7	34.8	375.9	21.4	31.0
Run3	50	JMA	0.6	820.6	85.4	492.4	28.9	34.6
Run4	75	JMA	0.9	820.6	85.4	738.5	43.3	34.6
Run5	60	CHI	0.9	884.4	70.6	796.0	34.6	57.7
Run6	100	JMA	1.2	820.6	85.4	984.7	57.7	34.6
Run7	50	CHI	0.7	884.4	70.6	619.1	28.9	57.7
Run8	125	TAK	1.0	605.5	124.2	605.5	72.2	23.1
Run9	70	CHI	1.0	884.4	70.6	884.4	40.4	57.7

earthquake recorded at Tohoku university in 1978, ELC, Imperial Valley earthquake recorded at EL Centro in 1940, JMA, Hyogo-ken Nanbu earthquake recorded at Japan Meteorological Agency in 1995, CHI, Chile earthquake in 1885, TAK, Hyogo-ken Nanbu earthquake recorded at Takatori station. The level of base motions were determined on the basis of preliminary analysis results, on the consideration of obtaining response data of walls in elastic, nearly yield point and up to ultimate state after yield point, the two specimens were subjected to the same series of base motions. Before and after the input of base motions, a white noise motion with small level was input to observe the change of the natural frequency of the damaged specimens.

RESULTS OF TEST

Damage process of specimen

Cracks condition in specimens after input, yield condition of reinforcements and natural frequency calculated from acceleration records at the base and top slab are observed. Natural frequency of specimens before damaged, Wall-A's was 10.25Hz, and Wall-B's was 8.06Hz. On Wall-A the shear crack occurred 45 degrees aslant nearly, on Wall-B the flexural share crack occurred from the lower column aslant to the opposite column, the difference in a crack between specimens can be showed. Specimens in the final state are shown in Fig.5: Wall-A after Run9 (CHI70), Wall-B after Run6 (JMA100)(figure after earthquake data name represent maximum target velocity). Ultimate collapse state on Wall-A, shear crack on center of first-story wall panel spread and wall panel crushed on the diagonal, follow that, lower column crushed. While on Wall-B, corner of wall panel crushed with lower column, the both collapse state was a little different. But level of maximum deformations are almost the same, both specimens were brittle failure type after bending yield.



Wall-A after Run9



Wall-B after Run6

Fig.5. Specimens and cracks appeared after test

Maximum strength

Fig.6 shows relations of equivalent height (height of subjecting inertia force)-shear strength of test and calculation. Shear strength were calculated by using Hirose's equation and shear strength equation in reference [2], where deflection angle of wall Ru apply 1/200 and 1/67, shear reinforcement ratio ($\rho_s=0.006$) consider effect of reinforcement of beam in calculating, and result of material test in Table2 and Table3 were used for material property. Shear force of test were lateral force that obtained by multiplying lateral acceleration distribution measured on top slab and weight by mass distribution. Shear force on flexural strength wQ_{mu} , which were calculated as divided flexural strength by equivalent height, is also shown in the graph.

Maximum shear force of Wall-A was 730kN at Run6 (JMA100), Maximum shear force of Wall-B was 578kN at Run4 (JMA75). Maximum shear force of Wall-B was about 80% as lower as that of Wall-A, due to equivalent height. And both observed shear force are as much as 120 percent of shear force on flexural strength wQ_{mu} . The cause of strength increase shown in the result can be attributed the strain effect of reinforcement, the accuracy of the formula, etc. Then shear strength were recalculated base on reference [3], considered strength rise of reinforcement strain rate were assumed 0.05 1/sec from the test data. As the results shear strength were 720kN (Wall-A) and 566kN (Wall-B), calculative and experimental results were in good agreement.

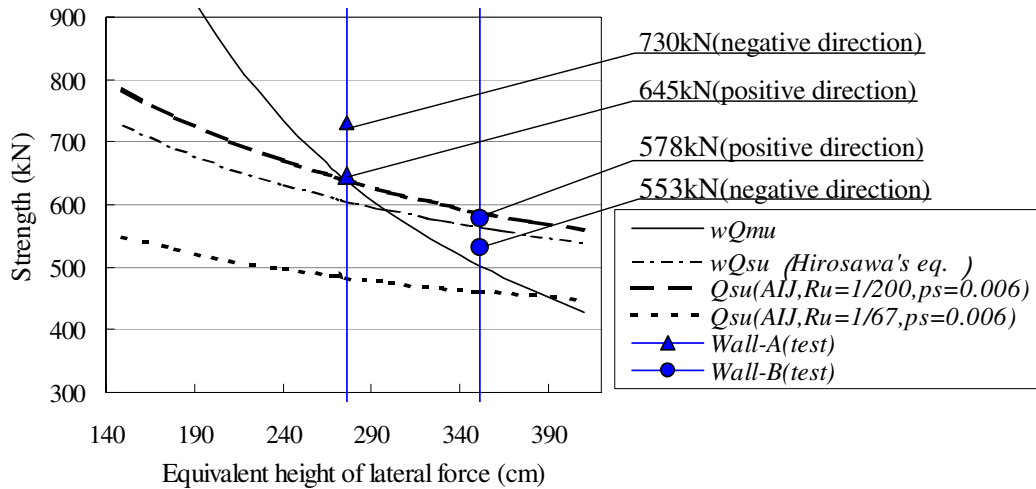


Fig.6. Shear strength of specimens

Relation of Lateral Force-Horizontal Displacement

Relations of Lateral force-horizontal displacement at top slab (height is 2m) of specimens are shown in Fig.7. Wall-A was in elastic stage to Run3 from Run1 nearly, showed stiffness degradation at Run4. While Wall-B was in elastic stage at run1 and Run2, showed stiffness degradation at Run3. Both specimens draw hysteresis of type as S-character, which energy absorbing capacity is low and residual displacement is small, up to reach maximum lateral force. Lateral force of Wall-A reached positive-direction maximum 645kN(deflection angle $R=1/248$), next negative-direction maximum 730kN ($R=1/121$) at Run6. After that, hysteresis curve moved to slip type with degradation of stiffness and strength of wall. Wall-A collapsed at Run9. As for Wall-B, Lateral force reached negative-direction maximum 533kN(deflection angle $R=1/248$), then positive-direction maximum 578kN ($R=1/208$). At input of Run5 after lateral force reached maximum, softening of strength was shown in figure. Then it collapsed at Run6. Deflection angle at yield point is near of $1/250$ in two specimens. Although deformation progressed gradually as hysteresis loop was repeated, deflection angle stopped progressing by about $1/100$. Two specimens didn't show the remarkable difference in hysteresis characteristic.

Consumption Energy

Consumption energy for flexural deformation, shear deformation and total deformation of specimens is shown in Fig.8. The flexural deformation is obtained by curvature, which is calculated from axial deformation of column by pieces of 4 parts. The shear deformation is deformation removed flexural deformation from total deformation. Consumption energy is area of hysteresis loop which is obtain by integrate lateral force by displacement at height of inertia force. Although input base motions were different between specimens, consumption energy of total deformation of both specimens is almost the same. The effect of input at Run5 (CHI60) after maximum shear force of Wall-B was reached was large.

Most of energy of Wall-B was consumed at Run5 (CHI60). At Run6 (JMA100) after that, Wall-B collapsed as soon as inputted, it is guessed that Wall-B have been in ultimate state at end of inputted Run5. Wall-B demonstrated big accumulation consumption energy capability in Run5 (CHI60) of long duration as a result of test, it is remarkable that Wall-B consumed as much accumulation energy as Wall-A until collapse.

As for flexural and shear deformation, it was found that shear deformation is about twice as much as flexural deformation in Wall-A. While two components of deformation occupy about the same amount of energy in Wall-B, so difference of deformability between both walls were shown.

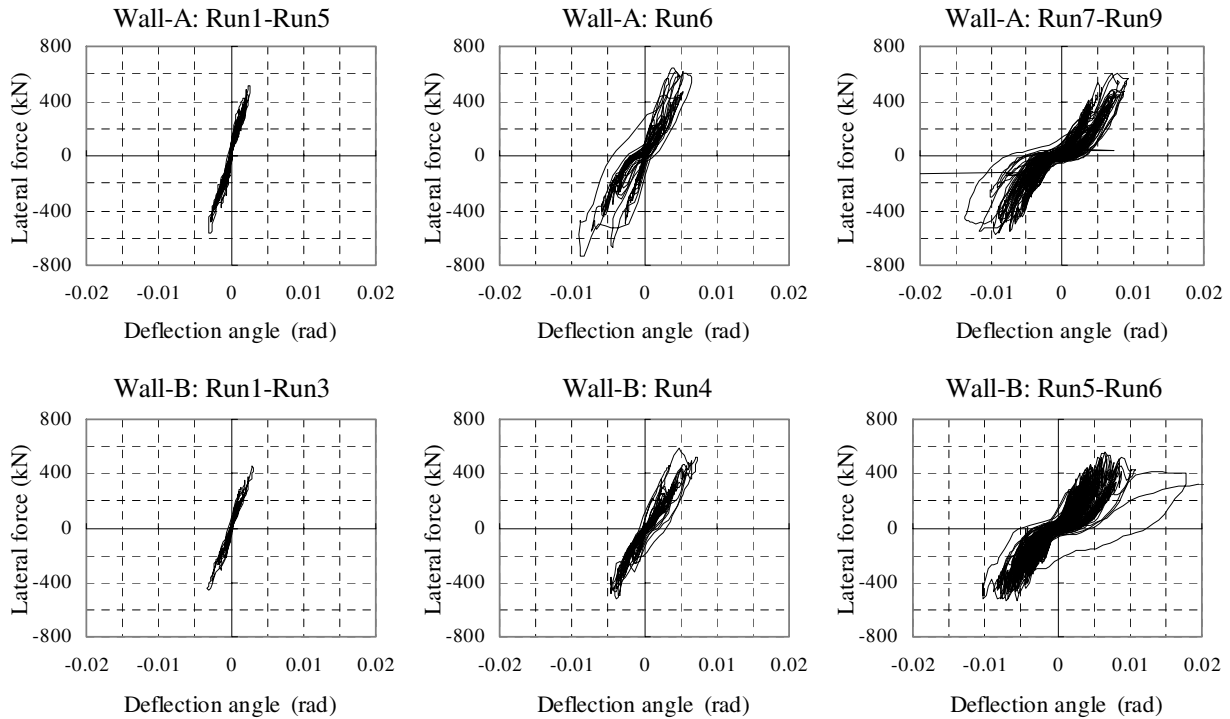


Fig.7. Relations of lateral force-Deflection angle (Deflection angle was measured top of walls, h=2m.)

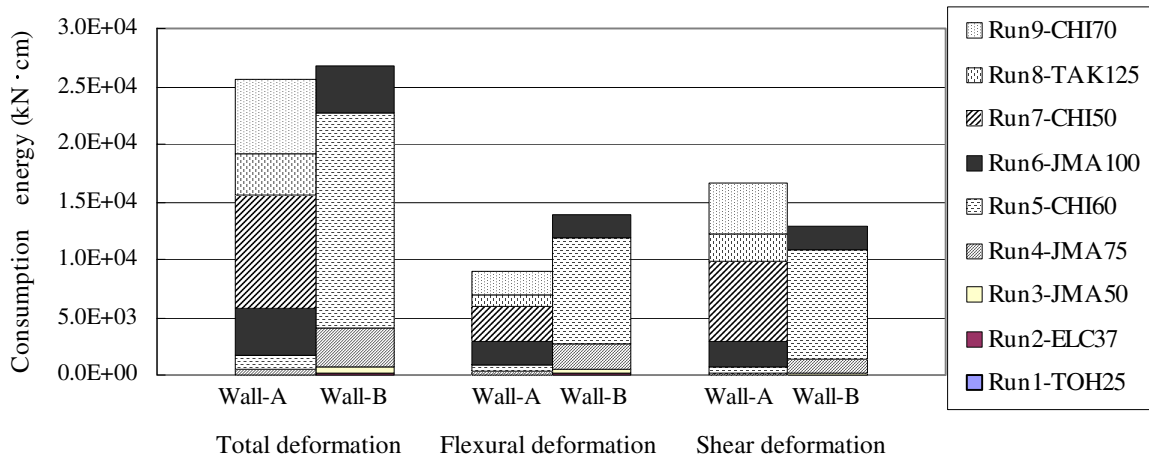


Fig.8. Consumption energy for components of deformation of shear wall

Ultimate deformation

Envelope curve of relations of lateral force-deflection angle is shown in fig.9. And, results of ultimate deflection angle observed from test data and calculated are drawn on the figure. The ultimate deflection angle from test data is deformation when lateral force declines to 80% of maximum, and the calculated result is deformation obtained by equation in reference [2], using the shear strength equal to 80 percent of measured maximum lateral force in test.

In Wall-B, the calculated deflection angle is greater than test value. This is may be caused by many cyclic responses in that deflection angle is $1/200\sim 1/100\text{rad}$, due to longer period input wave in post peak response, so that large amount of energy was dissipated in Wall-B, and Wall-B collapsed before the calculated deflection angle is achieved, as shown from consumption energy in former section.

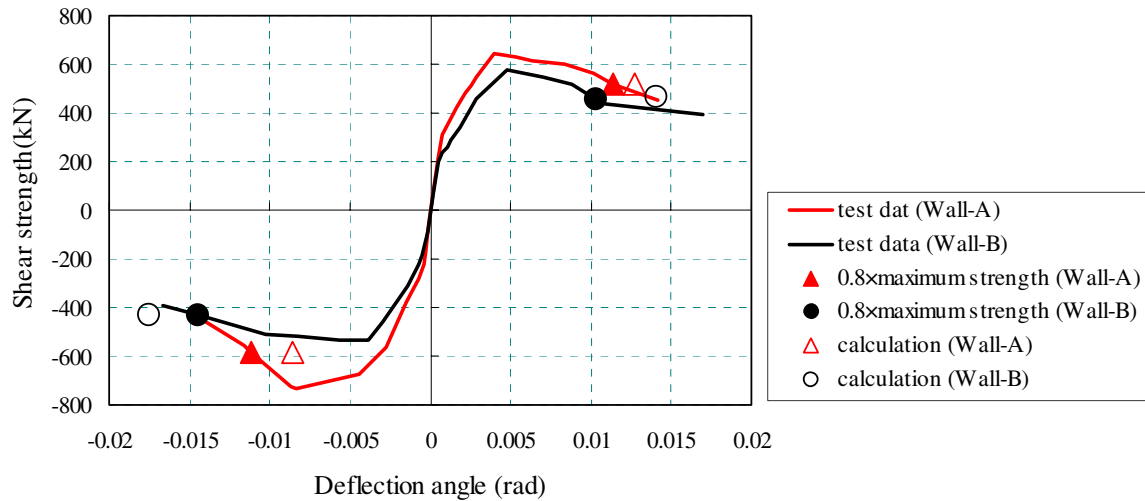


Fig. 9. Comparison of measured and calculated ultimate deformation

ANALYSIS OF SHEAR WALL

Description shear wall model

In this analysis, isoparametric element shear wall model developed by Chen [4] is used. This model composed of one isoparametric element and line elements. The reinforced concrete plate element model introduce smeared crack model, and it has been constructed by combining the constitutive law for concrete and that for reinforcement bars. These constitutive equations are given as the relationships between the average stress and average strain. It is assumed that reinforcement bars are distributed in the plate element, strain of concrete and reinforcement bars are equivalent. Crack model of concrete is rotating crack model. Rotating crack model has advantages of simplifying analytical program, because shear transfer model for fixed crack model is not needed and parameters on program could be reduced. However introduction to shear wall model and application under cyclic loadings is much less investigated so that further verification is needed (e.g. [5], [6]).

Constitutive law

The reinforced concrete plate element model has been constructed by combining the constitutive law for concrete and that for reinforcement bars. Relation of stress and strain for reinforced concrete is given as

$$\{\sigma\} = \{[Tc]^T [Dc][Tc] + [Ts]^T [Ds][Ts]\} \{\varepsilon\} = [D] \{\varepsilon\} \quad (1)$$

Where $\{\sigma\}$: average stress of reinforced concrete element, $\{\varepsilon\}$: average strain of reinforced concrete element, $[Dc]$: stiffness matrix of concrete in principal direction, $[Ds]$: stiffness matrix of steel in reinforcing bars direction, $[Tc]$: coordinate transformation matrix of concrete, $[Ts]$: coordinate transformation matrix of reinforcement bar.

Constitutive law for uncracked concrete is represented equation (2) based on constitutive law in a plain stress state. As for constitutive law for cracked concrete, it is assumed that, direction of crack and the direction normal to principal tensile strain are the same, as direction of principal tensile strain is change, direction of crack rotate, therefore principal axis of stress and strain are idealized to be the same anytime. From these assumption, constitutive law is represented equation (3).

Uncracked concrete:

$$[D_c] = \frac{E_c}{1-\nu^2} \begin{bmatrix} 1 & \nu & 0 \\ & 1 & 0 \\ sym & & (1-\nu)/2 \end{bmatrix} \quad (2)$$

Cracked concrete:

$$[D_c] = \begin{bmatrix} E_1 & 0 & 0 \\ & E_2 & 0 \\ sym & & G \end{bmatrix} \quad (3)$$

Where, E_c : elastic modulus of uncracked concrete, E_1, E_2 : secant modulus in direction of first and second principal strain, ν : Poisson's ratio of concrete, G : shear modulus due to crack.

And G of shear modulus is determined by equation (4) using Mohr's stress circle and strain circle from condition to satisfy assumption that direction of stress and strain are the same.

$$G = \frac{\sigma_1 - \sigma_2}{2(\varepsilon_1 - \varepsilon_2)} \quad (4)$$

Where, σ_1, σ_2 : principal stress due to crack concrete, $\varepsilon_1, \varepsilon_2$: principal strain due to crack concrete.

Considering just axial direction stiffness of steel, constitutive law of reinforcement bars is represented as

$$[D_s] = \begin{bmatrix} \rho_{sx} E_{sx} & 0 & 0 \\ & \rho_{sy} E_{sy} & 0 \\ sym & & 0 \end{bmatrix} \quad (5)$$

Where ρ_{sx}, ρ_{sy} : reinforcement ratio in x and y direction, E_{sx}, E_{sy} : secant modulus of reinforcement in x and y direction.

Material model for plate element

Concrete stress-strain model in compression introduced reduction factor suggested by Vecchio and Collins [7] to decrease the compressive strength of cracked concrete as a function tensile strain perpendicular to compressive strain. And stress-strain model for strain-softening is modeled by linear line. In tension, model by Okamura and Maekawa [8] is used. Bilinear-model is used for reinforcement.

Procedure of analysis

Analysis model of specimen is shown in Fig.10. The model is composed of plate element described in former section and line element of column and beam. Column is modeled by nonlinear spring model, considering only axial stiffness. And bending spring of beam is rigid and axial spring of that is linear. Specimens were subjected to load by given increment displacement at height of center of mass, on the other word, difference between two specimens are expressed by loading position. Unbalanced force due to changed stiffness is canceled at next step.

Results of analysis

Envelope curve of relationship between lateral force and deflection angle obtained from test and relationship between lateral force and rotating angle when cyclic load is applied to the shear walls are shown in Fig.11.

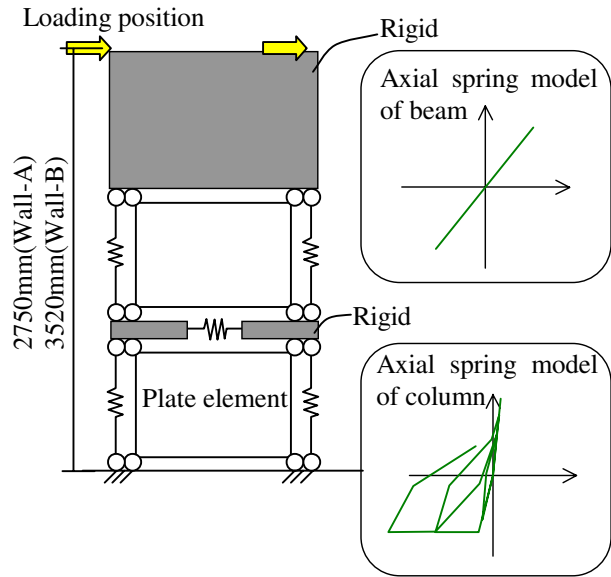


Fig. 10. Modeled specimen for analysis

The analytical initial stiffness and yield point in agree well with the experimental results in both specimens of Wall-A and Wall-B. And maximum strength forces of shear walls of test result to those of analytical result are 120 percent. As one cause, Strength rise due to reinforcement strain rate of is estimated one of cause for these. In fig.10 deflection angle when lateral force declines to 80% of maximum are plotted form result of analysis and experiment, respectively.

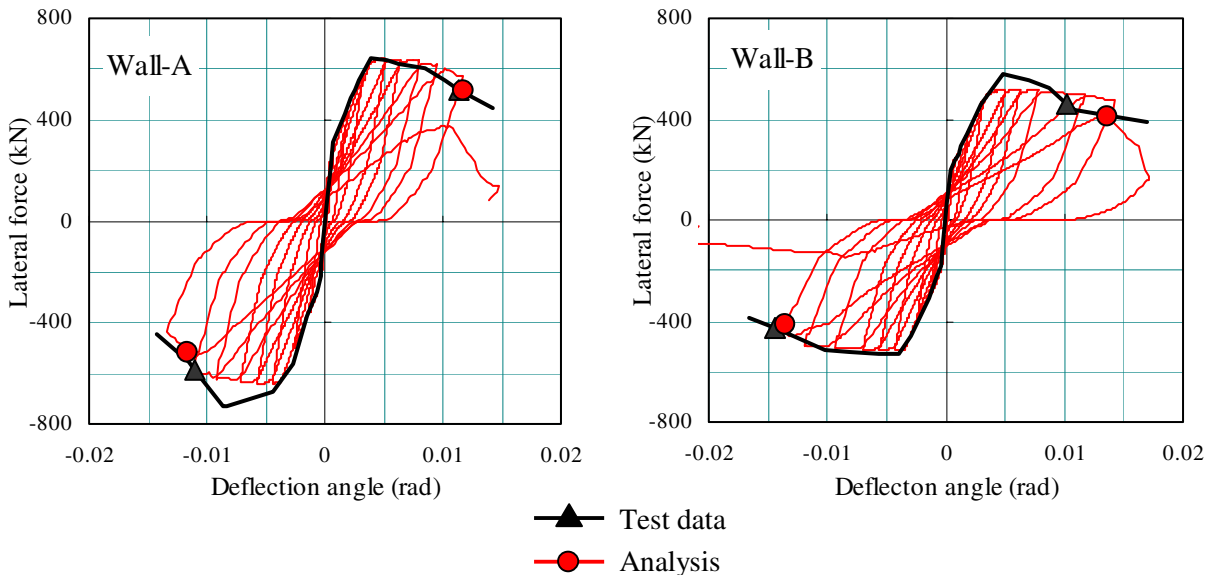


Fig.11. Relation of lateral force-reflection angle for test and analysis (Markers indicate point of 80% of maximum lateral force)

Although result of analysis is evaluated a little bigger than that of experiment in Wall-A, they are in good agreement. On the other hand, analytical result of Wall-B is 14×10^{-3} (rad) and experimental result is 10×10^{-3} (rad) in positive direction, that in negative direction are in well agreement.

CONCLUSION

A dynamic experiment of two reinforced concrete walls with different height of inertia force was carried out. The following can be draw form the result of the earthquake simulation tests and analytical result.

- (1) Both specimens failed in shear after flexural yielding. The failure mode was different: Wall-A in higher shear at flexural yielding failed in panel first, whereas Wall-B in low shear failed more in the boundary column. The deformability of Wall-B was not larger than expected from the design guidelines based on static tests.
- (2) Maximum shear force of Wall-B was about 80% as lower as that of Wall-A. Flexural strength of both specimens was higher than the calculated values due to the strain rate of reinforcement.
- (3) Both specimens showed pinching hysteretic behavior with low energy absorbing capacity and small residual displacement up to reach maximum lateral force. After that, hysteresis curve moved to slip type dominated by increasing shear deformation.
- (4) Wall-B demonstrated high energy dissipation capability in Run5 (CHI60) with long duration. As a result, Wall-B dissipated as much energy as Wall-A until collapse.
- (5) The envelope curve of the observed hysteresis relations with strength deterioration could be simulated well until up to shear failure by a macro member model that incorporated the effect of concrete strength softening under combined two-dimensional stresses.

ACKNOWLEDGEMENT

The study has been carried out as a part of “Special Project for Earthquake Disaster Mitigation in Urban Areas (DaiDaiToku project)” sponsored by MEXT, and the test was conducted on the large-size shaking table of NIED, Tukuba, in June and July 2002. Cooperative works of Makiko Ohi, SongTao Zhuang, graduate students, Kim Jin-Gon, research student, Univ. of Tokyo, Tomohusa Akita, Toyohashi Univ. of technology, Hideyoshi Watanabe, Sadayuki Ishizaki, Taisei Corporation, are gratefully acknowledged.

REFERENCES

1. AIJ. “Guidelines for Performance Evaluation of Earthquake Resistant Reinforced Concrete Building (Draft)”, Japan, 2003.
2. AIJ. “Design guidelines for earthquake resistant reinforced concrete building’s based on inelastic displacement concept”, Japan, 1997.
3. Satoshi IWAI, Nozomu YOSHIDA, Takeshi NAKAMURA and Minoru WATANABE, “Effect of loading rate on the performance of structural element -Part 1 Effect of strain rate on stress-strain relationship of concrete and steel-“ Transactions of the Architectural Institute of Japan, No.314. AIJ, Japan, 1982.4. pp.102-111.

4. Shaohua, C. and Toshimi KABEYASAWA, "Modeling of reinforced concrete shear wall under varying axial load", The 10th Earthquake Engineering Symposium Proceedings, Japan, 1998, G1-15, 1998. pp. 2363-2368.
5. Keisuke MIZUKI, Nobuaki SHIRAI, Kazuhito MORIIZUMI and Takahito Kojima, "Constitutive law for reinforced concrete element under cyclic in-plane stresses", Summaries of technical papers of Annual Meeting Architectural Institute of Japan. Structures II, AIJ, Japan, 1996.9. pp.487-490.
6. Atsushi YAMAYA, Hikaru NAKAMURA and Takeshi HIGAI. "Shear behavior analysis of RC beams using rotating crack model" Proceedings of JSCE, ASCE, No.620, V-43, 1999.5. pp.187-199.
7. Vecchio,F. and Collins,M.P. "The Modified Compression Field Theory for Reinforced Concrete Elements Subjected to Shear", ACI Journal, ACI, Vol.83, 1986. pp.219-231.
8. Hajime OKAMURA and Koichi MAEKAWA, "Nonlinear analysis and constitutive models of reinforced concrete", Giho-do Press, University of Tokyo, Japan, 1991.